대한기계학회 2001년도 춘계학술대회논문집 D pp. 181~188 KSME 01S423

FLOW BOILING HEAT TRANSFER FROM PLAIN AND MICROPOROUS COATED SURFACES IN SUBCOOLED FC-72

K. N. Rainey*, G. Li* and S. M. You**

Key Words : Flow Boiling, Microporous Coating, Nucleate Boiling Enhancement

Abstract

The present research is an experimental study of subcooled flow boiling behavior using flat, microporous-enhanced square heater surfaces in pure FC-72. Two 1-cm^2 copper surfaces, one highly polished (plain) and one microporous coated, were flush-mounted into a 12.7 mm square, horizontal flow channel. Testing was performed for fluid velocities ranging from 0.5 to 4 m/s (Reynolds numbers from 18,700 to 174,500) and pure subcooling levels from 4 to 20 K. Results showed both surfaces' nucleate flow boiling curves collapsed to one line showing insensitivity to fluid velocity and subcooling. The log-log slope of the microporous surface nucleate boiling curves was lower than the plain surface due to the conductive thermal resistance of the microporous coating layer. Both, increased fluid velocity and subcooling, increase the CHF values for both surfaces, however, the already enhanced boiling characteristics of the microporous coating appear dominant and require higher fluid velocities to provide additional enhancement of CHF to the microporous surface.

1. INTRODUCTION

It has been known for a long time that fully developed water nucleate flow boiling heat transfer performance in pipes is seemingly unaffected by either fluid velocity or subcooling (McAdams [1]). With regard to insensitivity to fluid velocity, Engelberg-Forster and Greif [2] explained that in both, forced convection and boiling heat transfer, the heat is first transferred to a thin layer of fluid adjacent to the surface. The heat is then transferred to the bulk liquid through diffusion by eddies in forced convection and/or through a bubble pumping or "vapor-liquid exchange" mechanism in boiling (commonly referred to as microconvection). This boiling microconvection mechanism was thought to be much more efficient due to the high departure frequency of bubbles and thus dominate the heat transfer over the eddy diffusion mechanism of forced convection.

With regard to insensitivity of nucleate flow boiling to fluid subcooling, Engelberg-Forster and Greif [2] believed that this behavior was due to the counterbalancing effects of subcooling on the maximum bubble size and the bubble departure frequency. Increased subcooling decreases the departing bubbles' size through condensation, which then decreases the amount of heated fluid it removes in its wake (decreased microconvection). From the results of Ellion [3], Engelberg-Forster and Greif also believed that the increased subcooling increases the bubble departure frequency, which helped to compensate for the decreased microconvection and thus show insensitivity to fluid subcooling. However, Yin, et al. [4] observed that increased subcooling reduces both, the bubble departure diameter and frequency for subcooled flow boiling of R-134a in an annular duct. Alternatively, Gunther [5] observed that departing bubbles would slide along the entire length of the heated wall before departing at high subcooling of water in a rectangular duct. Later, Bibeau and Salcudean [6] and Klausner et al. [7] observed similar sliding behavior in water and R-113, respectively. These more recent observations of bubble behavior in subcooled flow boiling suggest that increased bubble sliding, not increased bubble departure frequency, may be responsible for the compensation of decreased microconvection heat transfer as put forth by Engelberg-Forster and Greif.

More recently, Willingham and Mudawar [8] observed insensitivity of the entire nucleate boiling curve to both fluid velocity and subcooling in flow channels with small (10 mm × 10 mm), discrete heat sources in FC-72 for a velocity and subcooling range of 0.013 to 0.400 m/s and 3 to 36 K, respectively. Heindel et al. [9], and later Tso et al. [10], found similar results at high heat fluxes where fully developed nucleate boiling existed, however, they

* Department of Mechanical and Aerospace Engineering, University of Texas at Arlington
** School of Mechanical & Aerospace Engineering, Seoul National University

found a significant effect of both fluid velocity and subcooling at low heat fluxes due to partial boiling conditions. In contrast, Kirk et al. [11], using a larger (19 mm × 38 mm) thin film surface in R-113, found that increased fluid velocity increased heat transfer performance over the entire nucleate boiling curve for a velocity range of 0.04 to 0.325 m/s at 11.1 K subcooling. Samant and Simon [12] also found a significant effect of fluid velocity on the nucleate boiling curve of their thin film heater in FC-72, but at relatively high fluid velocities (4.1 to 9.3 m/s) and subcooling (≈55 K).

The effects of fluid velocity and subcooling on the critical heat flux (CHF) of small, discrete surfaces have also been previously studied. Kutateladze and Burakov [13] studied the effects of fluid velocity and subcooling on CHF for a vertical plate flow boiling in Dowtherm A (26.5% diphenyl and 73.5% diphenyl oxide). They observed that for a given velocity, CHF increases linearly with increasing subcooling and for a given subcooling, the CHF increases with increasing velocity for a velocity range of 1.2 to 5 m/s and a subcooling range of about 20 to 110 K. Using a very small (0.25 mm × 2.0 mm) thin film heater in FC-72, Samant and Simon [12] also found that CHF increased with increasing velocity for a velocity range of 2 to 17 m/s. In addition, Kutateladze and Burakov observed that the subcooling effect was more pronounced at higher velocities. Using a small rectangular surface (12.7 mm × 12.7 mm) in FC-72, Mudawar and Maddox [14] observed an increase in CHF with both increased velocity and subcooling and identified two distinct CHF regimes for low and high velocities. The transition from low to high velocity was characterized by an increase in the rate of CHF enhancement with velocity. This trend has also been observed by McGillis et al. [15], Willingham and Mudawar [8], and Tso et al. [10].

From pool boiling research it has been found that the microporous coating provides significant enhancement throughout the nucleate boiling curve (Chang and You [16,17]), however, its enhancement ability under flow boiling has not yet been determined. Therefore, the objective of the present research is to study the effects of fluid velocity and subcooling on the heat transfer performance from a microporous enhanced surface.

2. EXPERIMENTAL APPARATUS

2.1 Test Facility

The test section in Fig. 1 is constructed of Lexan, which allows for test heater visualization from both the side and top. The flow channel has a 12.7 mm × 12.7 mm square cross section and is 552 mm long. Although only one heater is tested at a time, the test section allows for the installation of two test heaters. The test heaters are located 400 and 464 mm (31.5 and 36.5 hydraulic diameters) from the test section inlet and are in the horizontal, upward facing orientation. The fluid flow at the test heaters is estimated to be fully developed turbulent flow for the present flow rate range. The test heaters are secured in the test section with clamps and are sealed using o-rings. To ensure proper inlet pressure control, a pressure transducer was installed 47 mm upstream of the first heater.

Test heater power is provided by a computer controllable DC power supply. A shunt resistor connected in series with the test heater and power supply, rated at 100 mV and 20 A, was used to determine the current in the electric circuit. The measured voltage drop across the test heater (along with the current measurement) was used to calculate power applied to the test heater. A computer controlled data acquisition system is used for test heater control as well as all temperature, pressure, voltage, and flowmeter measurements.

2.2 Test Heater

The test heater design is shown in Fig. 2. The heating element consists of thin tantalum and titanium nitride films. The heating element was sputtered onto a 0.5 mm thick oxidized silicon wafer along with copper for solder connections. The total heating element electrical resistance was about 25 Ω . The heating element side of the wafer was soldered to copper tape for the power lead connections while the other side of the wafer was soldered to the copper test surface. The test surfaces were cut from 1.5 mm thick solid copper plate with dimensions of 10 mm × 10 mm. The surface condition of the plain test surface was highly polished (mirror finish).

For the microporous coated heater, the coating used is the ABM coating (shown in Fig. 3) introduced by Chang and You [17]. The microporous coating technique was previously developed by O'Connor and You [18], further refined by Chang and You [16,17], and patented by You and O'Connor [19]. The coating is a surface treatment technique used to increase vapor/gas entrapment volume and active nucleation site density by forming a porous structure of about 0.1-1 μm size cavities that is approximately 50 μm thick. Detailed descriptions of the coating are provided by O'Connor and You [18] and Chang and You [16,17].

2.3 Test Procedure

In order to obtain accurate flow boiling test data, a sound degassing and test procedure must be developed.

Some of the common pitfalls in flow boiling research from discrete heat sources are: 1) allowing premature edge nucleation to skew the nucleate boiling curve and prevent the collection of accurate incipience data, 2) not properly degassing the test fluid, which can significantly alter the nucleate boiling curve (Collier [20]), and 3) not maintaining constant pressure at the test section inlet (maintaining constant test section outlet pressure causes significant scatter in the test data due to changing inlet pressure from the two-phase pressure drop). The authors believe that all of these potential problems have been successfully addressed with the present test section/heater design and test procedure.

The test heater heat flux was controlled by voltage input. After each voltage change (heat-flux increment), a 15-second delay was imposed before initiating data acquisition. After the delay, the computer repeatedly collected and averaged 125 base surface temperature measurements over 15 seconds until the temperature difference between two consecutive averaged temperature measurements for all thermocouples was less than 0.2 K. The test section at this point was assumed to be at steady state. After reaching steady state, heater surface and bulk fluid temperatures were measured and the heat flux was calculated. For heat flux values greater than ≈80% of CHF, instantaneous surface temperature was monitored for 45 seconds after each increment to prevent heater burnout. Each instantaneous surface temperature measurement was compared with the previous increment's average surface temperature. If a temperature difference larger than 20 K was detected, CHF was assumed and the power shut off. The CHF value was computed as the steady-state heat-flux value just prior to power supply shutdown plus half of the increment.

2.4 Experimental Uncertainty

Single-sample uncertainties for this study were estimated using the method of Kline and McClintock [21]. Fluid velocity uncertainty was estimated as 5.4% at 0.5 m/s and 2.1% at 2 and 4 m/s. Uncertainty in pressure measurements was estimated as 2.0%. Heat flux measurement uncertainty was estimated based upon the values of Rainey and You [22]. The heat flux uncertainty for the present test heater is estimated as 6.0% at both 20 and 60 W/cm^2 . In addition, temperature measurement uncertainty was estimated as ± 0.4 K.

3. RESULTS AND DISCUSSION

The present study is to understand the effects of fluid velocity and subcooling on nucleate boiling and CHF for both plain and microporous coated flat surfaces. The test surfaces are 1-cm^2 (10 mm × 10 mm) copper blocks flush mounted in the bottom of a rectangular, horizontally positioned flow channel. The heating surfaces, one highly polished and one microporous coated, are positioned in the horizontal, upward facing orientation and are intended to simulate a small microelectronic device. The fluid velocity and subcooling are varied from 0.5 to 2 m/s (Reynolds numbers from 18,700 to 174,500) and 4 to 20 K, respectively. The 2 m/s and 4 m/s cases at 4 K subcooling were not included in the reported results due to excessive inlet flow instability related to cavitations. All testing is performed in pure FC-72 at atmospheric pressure.

3.1 Pool Boiling Tests of Reference Surfaces

In order to qualify the present test heater surfaces, pool boiling curves in saturated FC-72 at atmospheric pressure were generated. Figure 4 illustrates the plain and microporous coated surfaces' pool boiling test results. For reference, the pool boiling tests were conducted in the same facility and with the same procedures used by Rainey and You [22]. The single-phase natural convection data of the present heaters exhibited comparable heat transfer coefficients showing negligible surface microstructure effects. Incipient superheat values ranged from 19 to 24 K for the plain surface and 4 to 8 K for the microporous coated surface showing the superior nucleation characteristics of the microporous coating. Throughout the nucleate boiling regime, the microporous coated surface consistently augmented heat transfer coefficients by more than 300% when compared to those of the plain surface. This enhancement is the result of the dramatically increased active nucleation site density caused by the surface microstructures provided by the microporous coating (O'Connor and You [18]). The CHF values for the plain surface ranged between 11.3 to 13.0 W/cm^2 while the microporous coated surface showed consistently enhanced CHF values of 23.5 W/cm^2 . In addition, these results are comparable to those reported by Chang and You [23] for their plain and microporous coated 1-cm^2 surfaces of similar construction.

3.2 Plain Surface Flow Boiling Results

The flow boiling curves of the plain surface are shown in Fig. 5 plotted versus ΔT_{bulk}. The single-phase, forced convection data clearly shows the effects of fluid velocity as indicated by the dashed trend lines. Boiling generally spread over the entire surface of the heater at incipience, however, there appeared to be a higher concentration of active nucleation sites near the

downstream edge indicating a slightly higher wall temperature. This active nucleation site density pattern appeared to be prevalent throughout the boiling curve. In addition, there appears to be no discernable trend in incipient superheat with respect to either fluid velocity or subcooling. This apparent insensitivity of incipience to inlet subcooling and velocity is consistent with the R-113 tube flow boiling results of Hino and Ueda [24] and the R-12 and R-114 tube flow boiling results of Celata et al. [25]. For a given fluid subcooling, the nucleate boiling data in Fig. 5 appear to follow one line. This insensitivity of the nucleate boiling heat transfer coefficient to fluid velocity shows that the nucleate boiling heat transfer mechanism completely dominates the heat transfer process for the range of fluid conditions tested.

By plotting the boiling curve data versus ΔT_{bulk} in Fig. 5, the effect of fluid subcooling on nucleate boiling heat transfer appears to be directly related to subcooling level. The data of Willingham and Mudawar [8] and Gersey and Mudawar [26] show a similar effect. There is also an interesting trend concerning the characteristic bend in the boiling curve near CHF. As the fluid velocity increases, the bend appears to diminish considerably. This may be due to increased disruption of the larger, secondary vapor layer above the surface causing instability in the vapor removal mechanism near CHF.

Detailed visual observations were made of the nucleate boiling behavior for the 2 m/s, 10 K subcooling case. After incipience, the nucleate boiling was characterized by very small bubbles departing and flowing parallel to the heater surface. Increasing the heat flux appeared to cause the departing bubbles to merge, forming a "blanket" of thin streams that would merge with other streams. As the heat flux approached CHF, the vapor removal was very chaotic with large, wavy vapor streams. A high-speed video camera was used to observe the CHF phenomena. For about one second prior to CHF, it appeared that large portions of the surface (up to 75%) would alternately be covered with vapor and then rewetted until, suddenly, the entire surface was covered with vapor. Although video was taken at 600 frames/sec, the final blanketing of the surface by the vapor was too fast to determine the initial origin on the surface of the dryout.

3.3 Microporous Surface Flow Boiling Results

The flow boiling curves of the microporous surface are shown in Fig. 6 plotted versus ΔT_{bulk}. The single-phase, forced convection data (indicated by the dashed trend lines) of the microporous surface are slightly worse than that of the plain surface data shown in Fig. 5 for all flow velocities tested, which appears to contradict the single-phase natural convection data shown in Fig. 4. Since O'Connor and You [18] estimated the effective thermal conductivity of the microporous coating layer to be very low (0.95 W/m· K), the degradation in the single-phase forced convection of the microporous surface is most likely due to the added conductive thermal resistance of the coating. This degradation effect was probably not observed in the single-phase natural convection data shown in Fig. 4 because the additional temperature drop from conduction through the coating was estimated to be within the experimental uncertainty for those low heat flux levels (much lower than those for forced convection). Similar to the plain surface, boiling spread over the entire surface of the heater at incipience, however, there was a much greater number of active nucleation sites than the plain surface and they appeared to be more evenly distributed. The bubbles departing the surface formed a relatively smooth layer of small discrete bubbles above the heater surface. The microporous surface maintains its superior nucleation characteristics when moving from pool to flow boiling. At the lower fluid velocities and subcoolings, the nucleate boiling heat transfer coefficients of the microporous surface are still much better than those of the plain surface, however, at higher velocities and subcoolings, the reduction in slope of the microporous boiling curves causes the enhancement to disappear. The reason for this degradation in microporous surface performance is explained later. As with the plain surface, the microporous nucleate boiling data in Fig. 6 appear to follow one line for a given fluid subcooling showing the same insensitivity of the nucleate boiling heat transfer coefficient to fluid velocity. It is also interesting to note that there is virtually no bending in the microporous boiling curves near CHF as seen in the lower velocity plain surface data in Fig. 5.

Visual observations of the 2 m/s, 10 K subcooling case showed a slightly different boiling behavior for the microporous surface compared to the plain surface. As previously mentioned, the departing bubbles from the microporous surface formed a relatively smooth bubble layer above the heater surface after incipience. However, as the heat flux increased, the bubble layer remained smooth and stable unlike the plain surface, changing only in its thickness. About one second prior to CHF (using the high-speed video camera), the amount of vapor exiting the surface began to pulse rapidly. Once CHF was reached, the pulsing stopped indicating complete dryout of the heater surface.

3.4 Correlation of Flow Boiling Data

Figure 7 shows all of the plain and microporous boiling curves plotted versus ΔT_{sat}. The single-phase forced convection data have been removed for clarity.

The most striking feature of this graph is how both surfaces' nucleate boiling curves collapse to one line showing insensitivity of the nucleate boiling heat transfer to both fluid velocity and subcooling. The plain surface data are well correlated with the following equation:

$$q'' = 5.39 \cdot \Delta T_{sat}^{3.63}. \quad (1)$$

Equation (1) was found by fitting all of the nucleate boiling data excluding the bending portions prior to CHF. The log-log slope of 3.63 from Eq. (1) is similar to that observed by Willingham and Mudawar [8] (slope ≈3.7) and Gersey and Mudawar [26] (slope ≈3.5). Both of these references used 10 mm × 10 mm flat copper heaters in FC-72 at atmospheric pressure.

As can be seen in Fig. 7, the plain surface saturated pool boiling curve has a slope similar to the plain surface subcooled flow boiling curves but is shifted significantly to the right. This suggests that the boiling heat transfer performance is significantly affected by either fluid velocity or subcooling or both somewhere in the low velocity range between 0 to 0.5 m/s. Using a highly polished thin gold film heater in R-113, Kirk et al. [11] found that increasing fluid velocity from 0.041 to 0.325 m/s significantly shifted the entire nucleate boiling curve to the left by about 5 K. Further, Willingham and Mudawar [8] observed a negligible effect of fluid subcooling (3 to 36 K) on the flow boiling heat transfer from a vapor-blasted copper surface at a fluid velocity of 0.50 m/s in FC-72. In contrast, both Heindel et al. [9] and Tso et al. [10] found a significant effect of both subcooling and velocity at low heat fluxes due to partial boiling conditions. Since the partial boiling conditions described by Heindel et al. and Tso et al. were not observed in the present study, the observations of Kirk et al. and Willingham and Mudawar seem to suggest that the transition from pool boiling to subcooled flow boiling seen in the present plain surface data is primarily due to fluid velocity effects, however, more testing in this velocity range is needed before any conclusions can be made.

The microporous surface flow boiling data in Fig. 7 are well correlated by the following equation:

$$q'' = 1.94 \times 10^4 \cdot \Delta T_{sat}^{1.02}. \quad (2)$$

The microporous surface boiling curves also show a transition in heat transfer performance from pool boiling to flow boiling. From Fig. 7, it appears that the transition of the microporous surfaces is caused by fluid subcooling alone and is only significant in the lower heat flux region of the boiling curves. The microporous coating provides nucleate boiling enhancement by increasing the number of active nucleation sites at low heat fluxes (O'Connor and You [18]). It is hypothesized that the increased number of bubbles generated by the coating causes increased blockage to the fluid rewetting the surface. Increased fluid subcooling would reduce the bubble sizes through condensation and thus decrease the amount of blockage seen by the fluid allowing for more forced convection heat transfer. As the heat flux (and velocity) is increased, the effect of subcooling on the nucleate boiling heat transfer disappears.

Compared to the plain surface data, the microporous surface data in Fig. 7 have a much lower slope. In fact, above a heat flux of about 50 W/cm², the microporous coating actually provides worse heat transfer performance than the plain surface. It is postulated that this is caused by the apparent conductive thermal resistance of the microporous coating layer in the nucleate boiling situation (coating plus fluid within cavities) previously mentioned. To help explain this, the average surface heat transfer coefficients of all the boiling curves from Fig. 7 are plotted versus ΔT_{sat} in Fig. 8. The heat transfer coefficients calculated from Eqs. (1) and (2) are also plotted in Fig. 8. Very simply, the total thermal resistance for the plain heater is dependent only on the thermal resistance of flow boiling (latent heat and convection heat transfer), $R_{tot} = R_{boil}$, while the total thermal resistance for the microporous heater is dependent on the thermal resistance of flow boiling plus the thermal resistance of conduction for the thin microporous coating layer, $R_{tot} = R_{boil} + R_{cond}$. Since R_{cond} may be constant, this places a lower limit on R_{tot} for the microporous surface as R_{boil} becomes smaller at higher fluid velocities and subcoolings. Referring to Fig. 8, the nearly constant h-value ($\approx 2\times10^4$ W/m²·K) for the microporous surface means that $R_{boil} << R_{cond}$. From this realization, the effective thermal conductivity of the present (ABM) microporous coating layer can be estimated from $R_{tot} \approx R_{cond}$ as 1 W/m·K (coating thickness = 50 μm), which compares well with the values of 1.08 W/m·K estimated by O'Connor et al. [27] for their DOM microporous coating and 0.95 W/m·K estimated by O'Connor and You [18] for their silver flake microporous coating. It should also be noted that both O'Connor et al. and O'Connor and You compared pool boiling data of different coating thickness to determine their thermal conductivities, which is different from the present method. It is also interesting to observe that the maximum heat transfer coefficient seen in pool boiling on the microporous surface is also the maximum for subcooled flow boiling. The previously discussed transitions from pool to flow boiling for both surfaces can also be seen in Fig. 8.

3.5 Critical Heat Flux Behavior

The fluid velocity and subcooling effects on CHF for the plain and microporous surfaces are presented in Fig. 9. Both surfaces in Fig. 9 show significant enhancement of CHF with both increased fluid velocity and subcooling. The positive effect of fluid subcooling on CHF has already been noted by many researchers

(Mudawar and Maddox [14], Tso et al. [10]) and is due to a reduction, by condensation, in vapor covering the heater surface, which decreases the resistance to the liquid rewetting the surface and delays CHF. With respect to fluid velocity, the plain surface data show a change in slope near 2 m/s similar to that observed by Mudawar and Maddox [14]. Using Haramura and Katto's [28] macrolayer dryout model, Mudawar and Maddox explained that the low velocity CHF was caused by dryout of the liquid sublayer beneath a large continuous vapor blanket near the downstream edge of the heater. In the high velocity CHF regime, they observed that the thin vapor layer covering the surface was broken into continuous vapor blankets much smaller than the heater surface. This most likely decreases the resistance to the fluid rewetting the liquid sublayer, providing an additional enhancement to CHF and subsequent increase in slope as seen in Fig. 9. The dashed line in Fig. 9 represents the transition line proposed by Mudawar and Maddox to separate low and high velocity behavior. The microporous surface CHF values show this behavior as well, but to a lesser degree.

The lower slope of the microporous data compared to the plain surface data in Fig. 9 shows reduction in CHF enhancement as velocity increases similar to the reduction in nucleate boiling enhancement of the microporous surface previously discussed. Figure 10 shows the ratio of the microporous surface CHF data to the plain surface CHF data versus fluid velocity at ΔT_{sub} = 10 and 20 K. From Fig. 10 it can be seen that the microporous coating's effectiveness of enhancing CHF decreases linearly with increasing fluid velocity. In addition, from Fig. 10, it can be seen that increased subcooling causes a proportional increase in CHF, but the rate of reduction in CHF enhancement of the microporous coating with velocity appears to be the same.

Comparing the saturated pool boiling CHF values of the plain and microporous surfaces in Fig. 4 to their corresponding CHF values for the 0.5 m/s, 4 K subcooled flow boiling case reveals an interesting observation. The plain surface CHF increased by 36% when moving from saturated pool boiling to 0.5 m/s, 4 K subcooled flow boiling while the microporous surface CHF remained virtually unchanged. This suggests that the microporous coating already provides a more dominant nucleate boiling heat transfer mechanism, which requires higher fluid velocities than the plain surface to provide further enhancement of CHF.

4. CONCLUSIONS

To understand the effects of fluid velocity and subcooling on nucleate boiling and CHF from a microporous enhanced surface, two 1-cm² (10 mm × 10 mm) copper test surfaces were flush-mounted in the bottom of a rectangular, horizontally positioned flow channel. The heating surfaces, one highly polished and one microporous coated, are intended to simulate small microelectronic devices. The fluid velocity and subcooling were varied from 0.5 to 2 m/s and 4 to 20 K, respectively. All testing was performed in pure FC-72 at atmospheric pressure.

1) Both plain and microporous surfaces showed insensitivity to fluid velocity and subcooling level within the subcooled flow boiling ranges tested. The plain and microporous nucleate flow boiling curves collapsed to one line and were well correlated by Eq. (1) and (2).
2) The plain surface nucleate boiling heat transfer performance was significantly affected by fluid velocity and/or subcooling between 0 and 0.5 m/s and 0 to 4 K. The microporous surface was significantly affected by fluid subcooling at low heat flux levels for the lowest velocity tested (0.5 m/s); however, the behavior disappears with increased velocity and/or heat flux.
3) The log-log slope of the nucleate flow boiling curve for the microporous surface was much lower than for the plain surface and actually provided worse heat transfer performance than the plain surface above a heat flux of about 50 W/cm². This degradation in heat transfer performance of the microporous surface was caused by the limiting effect of the thermal resistance of conduction for the microporous coating layer.
4) The CHF values of the plain surface, increased with increasing fluid velocity and subcooling. The log-log slope of CHF versus fluid velocity significantly increased at about 2 m/s. The microporous surface showed similar behavior

REFERENCES

(1) McAdams, W. H., 1954, Heat Transmission, McGraw-Hill, New York.
(2) Engelberg-Forster, K. and Greif, R., 1959, ASME JHT, Vol. 81, No. 1, pp. 43-53.
(3) Ellion, M. E., 1954, "A Study of the Mechanism of Boiling Heat Transfer," Memo No. 20-88, California Institute of Technology, p. 72.
(4) Yin, C. P., Yan, Y. Y., Lin, T. F., and Yang, B. C., 2000, IJH&MT, Vol. 43, No. 11, pp. 1885-1896.
(5) Gunther, F. C., 1951, ASME JHT, Vol. 73, No. 2, pp. 115-123.
(6) Bibeau, E. L., and Salcudean, M., 1994, IJH&MT, Vol. 37, No. 15, pp. 2245-2259.
(7) Klausner, J. F., Mei, R., Bernhard, D. M., Zeng, L. Z., 1993, IJH&MT, Vol. 36, No. 3, pp. 651-662.
(8) Willingham, T. C., and Mudawar, I., 1992, IJH&MT, Vol. 35, No. 8, pp. 1865-1880.
(9) Heindel, T. J., Ramadhyani, S., and Incropera, F. P., 1992, ASME JEP, Vol. 114, No. 1, pp. 63-70.
(10) Tso, C. P., Tou, K. W., and Xu, G. P., 2000, International Journal of Multiphase Flow, Vol. 26, No.

3, pp. 351-365.
(11) Kirk, K. M., Merte, H. Jr, and Keller, R., 1995, ASME JHT, Vol. 117, No. 2, pp. 380-386.
(12) Samant, K. R., and Simon, T. W., 1989, ASME JHT, Vol. 111, No. 4, pp. 1053-1059.
(13) Kutateladze, S. S., and Burakov, B. A., 1969, "The Critical Heat Flux for Natural Convection and Forced Flow of Boiling and Subcooled Dowtherm," Pergamon, Oxford, pp. 63-70.
(14) Mudawar, I, and Maddox, D. E., 1989, IJH&MT, Vol. 32, No. 2, pp. 379-394.
(15) McGillis, W. R., Carey, V. P., and Strom, B. D., 1991, ASME JHT, Vol. 113, No. 2, pp. 463-471.
(16) Chang, J. Y., and You, S. M., 1997, IJH&MT, Vol. 40, No. 18, pp. 4437-4447.
(17) Chang, J. Y., and You, S. M., 1997, IJH&MT, Vol. 40, No. 18, pp. 4449-4460.
(18) O'Connor, J. P., and You, S. M., 1995, ASME JHT, Vol. 117, No. 2, pp. 387-393.
(19) You, S. M. and O'Connor, J. P., 1998, "Boiling Enhancement Paint," U. S. Patent #5814392.
(20) Collier, J. G., 1981, Convective Boiling and Condensation, 2nd ed., McGraw-Hill, New York.
(21) Kline, S. J., and McClintock, F. A., 1953, "Describing Uncertainties in Single-Sample Experiments," Mechanical Engineering, Vol. 75, No. 1, pp. 3-8.
(22) Rainey, K. N. and You, S. M., 2000, ASME JHT, Vol. 122, No. 3, pp. 509-516.
(23) Chang, J. Y. and You, S. M., 1996, ASME JHT, Vol. 118, No. 4, pp. 937-943.
(24) Hino, R. and Ueda, T., 1985, International Journal of Multiphase Flow, Vol. 11, No. 3, pp. 269-281.
(25) Celata, G. P., Cumo, M., and Setaro, T., 1992, Experimental Heat Transfer, Vol. 5, No. 4, pp. 253-275.
(26) Gersey, C. O., and Mudawar, I., 1992, ASME JEP, Vol. 114, No. 3, pp. 290-299.
(27) O'Connor, J. P., You, S. M., and Price, D. C., 1995, IEEE Trans. CPMT, Part A, Vol. 18, pp. 656-663.
(28) Haramura, Y., and Katto, Y., 1983, IJH&MT, Vol. 26, No. 3, pp. 389-399.

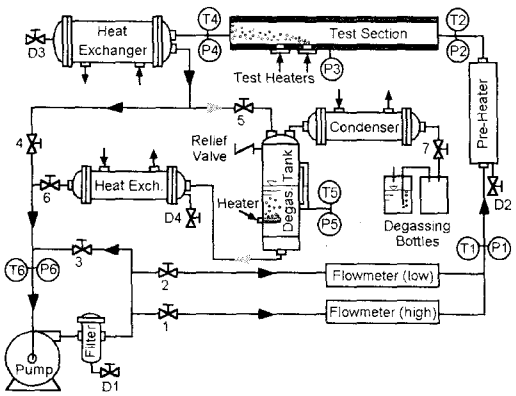

Fig. 1. Flow boiling test loop schematic.

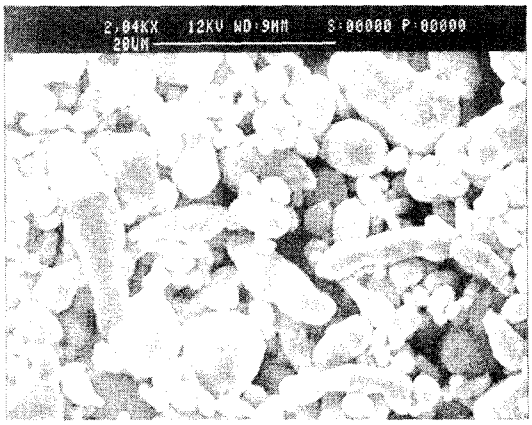

Fig. 3. SEM image of ABM microporous coating (top view).

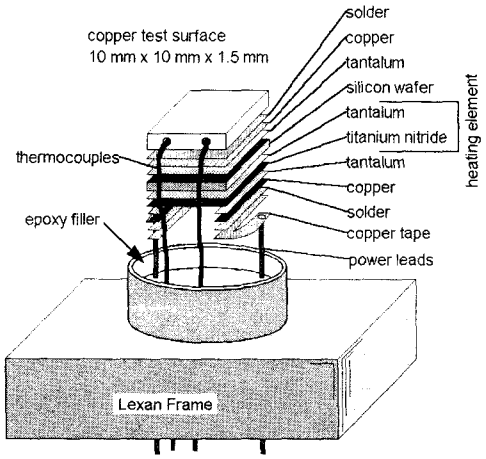

Fig. 2. Flow boiling test heater assembly.

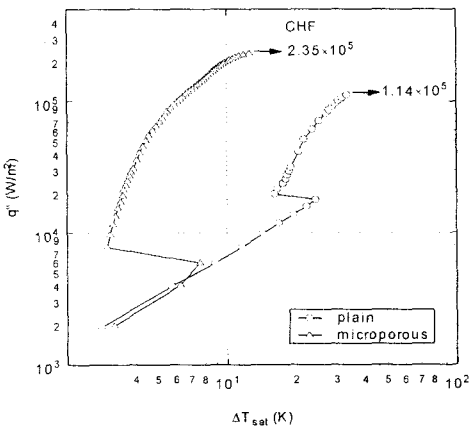

Fig. 4. Reference pool boiling curves.

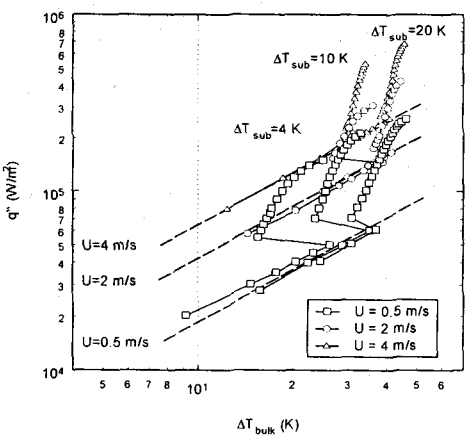

Fig. 5. Flow boiling curves of plain surface.

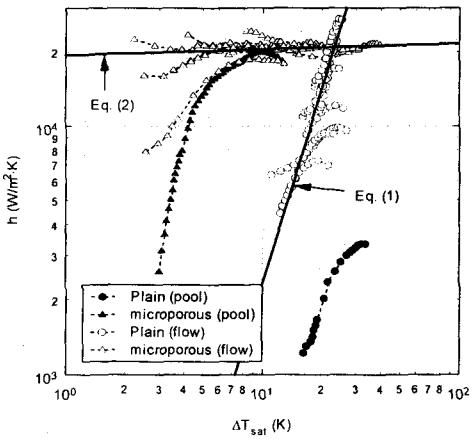

Fig. 8. Average nucleate boiling heat transfer coefficients.

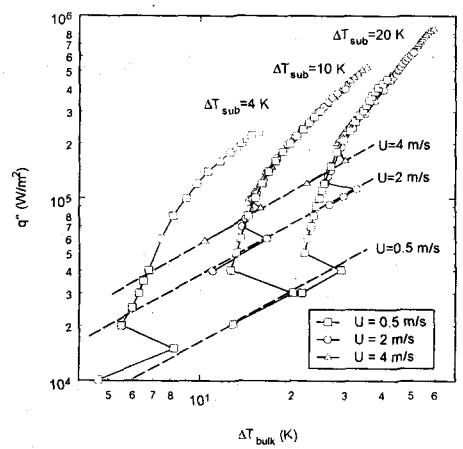

Fig. 6. Flow boiling curves of microporous surface.

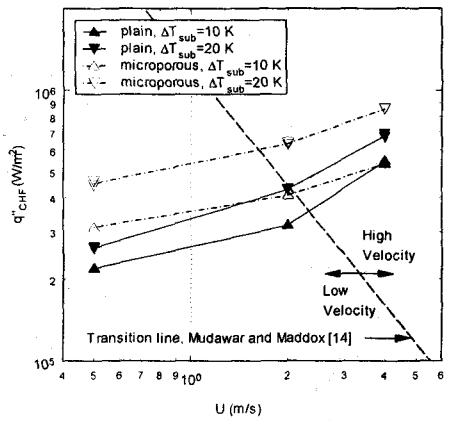

Fig. 9. Effect of velocity and subcooling on CHF.

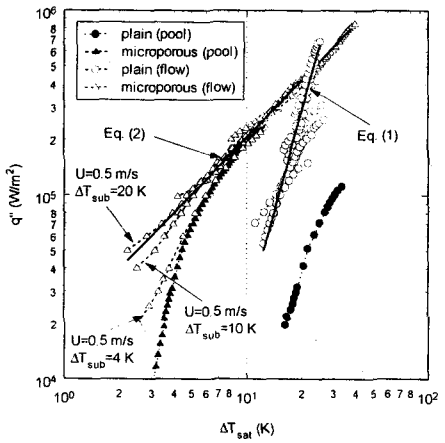

Fig. 7. Correlation of nucleate boiling curves.

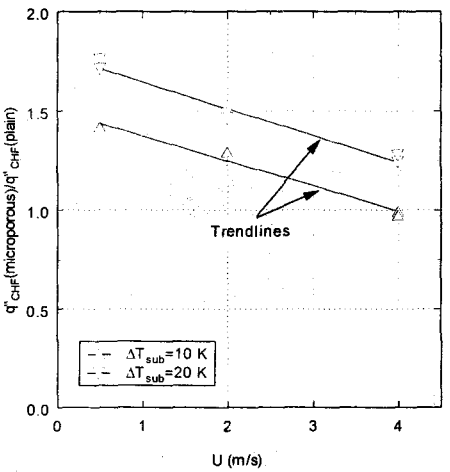

Fig. 10. Effect of velocity and subcooling on microporous coating effectiveness.